University of Groningen

A SIMPLE NUMERICAL ALGORITHM FOR ELASTOHYDRODYNAMIC LUBRICATION, BASED ON A DYNAMIC VARIATION PRINCIPLE

Verstappen, R.

Published in:
Journal of computational physics

IMPORTANT NOTE: You are advised to consult the publisher's version (publisher's PDF) if you wish to cite from it. Please check the document version below.

Document Version
Publisher's PDF, also known as Version of record

Publication date:
1991

A Simple Numerical Algorithm for Elastohydrodynamic Lubrication, Based on a Dynamic Variation Principle

R. VERSTAPPEN*

Department of Applied Mathematics, University of Twente,
P.O. Box 217, 7500 AE Enschede, The Netherlands

This paper deals with an efficient numerical method for the fully lubricated line contact between a rotating, deformable cylinder and a rigid surface. By exploiting the dynamic variation structure of this non-linear problem the deformation of and the pressure at the free, contact boundary are calculated. The dynamic formulation leads in a natural way to an iterative procedure, where the evolution from one iterate to a subsequent one is governed by a minimization problem. Physically, the Euler–Lagrange equation expresses the fact that the mass has to be conserved. For this reason, in contrast with earlier approaches, mass flux defects do not occur here. The proposed dynamic algorithm starts with the calculation of the lubricated contact between a rigid cylinder and the rigid surface. Then the stiffness of the cylinder is lessened until the desired value is reached, where after the loading on the cylinder is increased by moving it towards the rigid surface. The effort to proceed in time is significantly reduced by preconditioning: the discretized Euler–Lagrange equation is multiplied by an approximation of the inverse of the global operator governing the deflection of the cylinder. In this way, solutions that are comparable to large-time (or super-) computer computations can be calculated on a PC. © 1991 Academic Press, Inc.

1. INTRODUCTION

The use of lubricant to reduce the friction between two bodies in relative motion induced by a force pressing them together was recorded as early as 2400 B.C. (see [1]). *Elastohydrodynamic lubrication* (abbreviated EHL) theory studies this phenomenon in the ideal case that the (perfectly smooth) surfaces are fully separated by a thin fluid layer by regarding both the viscous flow of the lubricant and the elastic deformation of the bodies.

This paper deals with simple, efficient numerical calculations (based on the dynamic variation structure), that can be performed on a small PC with results comparable to large-time computer computations.

A simplified description of the flow field has been proposed by Reynolds in 1886 and the effect of the elastic distortion was considered some decades later. This led to the meanwhile classical Reynolds–Hertz model consisting of a second-order, non-linear differential equation involving the pressure at the deformed surface and

* Present address: University of Groningen, Department of Mathematics, P.O. Box 800, 9700 AV Groningen, The Netherlands.

the fluid-film thickness only, and an integral relation between these two quantities. Various numerical methods for solving this problem have been reported since the sixties. This development started with the inverse method of Dowson and Higginson [2]. The algorithms proposed more recently can roughly be classified as being either Newton–Raphson (cf. Oh [3]) or Gauss–Seidel methods (cf. Hamrock and Jacobson [4]). The Newton–Raphson algorithm linearizes the differential equation, while the non-linearity is frozen and now and then updated in the Gauss–Seidel approach. Recently, the convergence of the Gauss–Seidel relaxation is speeded up by using a multi-grid technique (see Lubrecht [5]).

In this paper, a different approach is presented. It is based on a new, dynamic variation principle, where the Euler–Lagrange equation governs the time evolution of the balance of mass. The dynamic iteration requires moderate computer facilities. In the present approach it is implemented on a personal computer and an average complete calculation takes some 5 min.

Nowadays, the advantages of variational formulations and allied finite element techniques are evident in solid mechanics, but have not quite been so impressive in fluid mechanics, in general. The main reason may be that convection and dissipation cannot be described by a unified variational principle. However, in standard EHL theory the effect of convection is always neglected compared to the viscous dissipation. From an engineering point of view this approximation is completely satisfactory (see, e.g., [6]). This basic assumption opens the door to the variational formulation of EHL theory.

To make this paper self-contained, this formulation is outlined in Section 2 (for a more detailed discussion the reader is referred to [7 or 8]). It combines the separate variational principles for the elastic deformation of the cylinder and that for the creeping flow of the lubricant. As usual, the elastic deformation corresponds to a state for which the elastic energy $\mathscr{E}$ is minimal, and the equilibrium state in the fluid is governed by the minimum of a power functional $\mathscr{P}$. Starting from these sound physical principles a unified formulation can be derived. This formulation is such that the total power $\mathscr{P} + d_t \mathscr{E}$ of the lubricated system is minimal.

The dynamic variation principle is used as a guid line for deriving a simplified formulation as well as for obtaining numerical solutions. Stated more, explicitly, the following two approximations are made within the variational formulation: (i) The (usual) approximations leading to the Reynolds–Hertz model. This leads to a simplified formulation containing only quantities for and at the deformed surface of the cylinder. This is, by construction, still a dynamic variation principle. (ii) The discrete representation of the variables, i.e., limiting the time to a discrete set of values and replacing the space of admissible variations by a finite dimensional subspace.

Compared to the earlier numerical works, the iteration has a different character. In Section 3, the iteration is viewed as a discrete time path. The evolution of this path is governed by the minimum of the discrete power functional. In terms of the parameters of the admissible subspace of variations, this minimum is described by a linear system of equations (Section 4).

   Usually, the distance between the centre of the deformed cylinder and the rigid surface is smaller than the radius of the undeformed cylinder. For this reason, the dynamic algorithm to follow starts with a rigid cylinder that is not in (dry) contact with the surface. Then the stiffness of the cylinder is lessened until the desired value is reached, whereupon the cylinder is moved towards the rigid surface. The velocity of this motion is limited by the requirement that the surfaces remain fully separated by the lubricating film (Section 5).

   The effort to proceed in time, that is to solve the minimization problem describing the evolution form one iterate to a subsequent one, is significantly reduced by multiplying the linear system with an approximation of the inverse of the global operator governing the deflection of the cylinder. The use of this preconditioner concentrates the weight of the matrix around the diagonal and allows for an approximation by a quasi-pentadiagonal matrix (Section 6).

   Some results obtained by the dynamic variation method are given in Section 7. Finally, the dynamic variation principle for EHL is extended to incorporate lubricants having a pressure-dependent viscosity (Section 8). The fundamental difficulty arising in this, is that the pressure cannot be viewed as a Lagrange multiplier which takes account for the balance of mass. Here, and ad hoc solution of this problem will be given: the viscosity is simply evaluated at a previous time level. Then, with minor changes, the algorithm for constant viscosity can be used again. A more fundamental treatment of an EHL problem with a pressure-dependent viscosity will be given in a forthcoming paper.

2. THE DYNAMIC VARIATION PRINCIPLE

   This discussion on elastohydrodynamic lubrication theory is limited to the lubricated *line contact* between a deformable, rotating cylinder and a rigid surface (see Fig. 1). The cylinder is so long that both the deformation of the elastic medium and the fluid are independent of the axial direction and have no component in this direction.
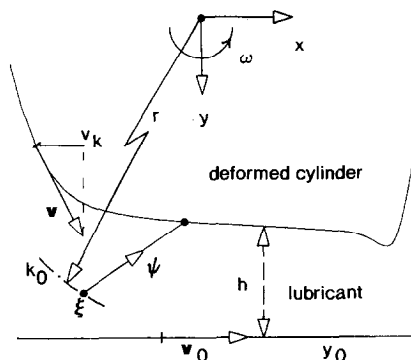

FIG. 1.   The configuration.

The Flow of the Lubricant

The deformation of the incompressible, Newtonian lubricant that leads to a thin film which separates the deformed cylinder from the rigid surface, is described by a sufficient smooth, orientation preserving, invertible mapping

$$\phi: \Sigma_0 \to \Sigma.$$

The motion of a label $\xi \in \Sigma_0$ is given by the curve $t \to \phi(\xi, t)$. In the *Lagrangian* view the velocity $\partial_t \phi(\xi, t)$ of this motion is attributed to the reference position ξ. Although this conception is formally correct, a fluid is usually not though of as to have a well-defined reference configuration, that can be detected in a physical experiment. Therefore a fluid is described in the *Eulerian* setting. That is, the velocity $v(x, t)$ is defined as the derivative $\partial_t \phi$ evaluated at the *current* position $x = \phi(\xi, t)$ of the label ξ:

$$\mathbf{v} = \partial_t \phi \circ \phi^{-1}.$$

In the following, *stationary* velocity fields will be considered. It is to be emphasized that this does *not* imply that the deformation ϕ is independent of the time t.

The fluid film is supposed to be homogeneous as long as the pressure p exceeds the cavitation pressure p_{cav}, which value may be normalized by setting $p_{\text{cav}} = 0$. By assumption, the flow of the lubricant is dominated by the viscous forces. Consequently, the equations in the interior of the physical domain Σ (which is confined to $p > 0$) can be obtained from the power functional

$$\mathscr{P}(p, \mathbf{v}) = \iint_\Sigma \left(\frac{\mu}{2} (\nabla_x \mathbf{v} + \nabla_x \mathbf{v}^T) : \nabla_x \mathbf{v} - p \, \text{div}_x \mathbf{v} \right) dx. \tag{1}$$

Here, the constant μ denotes the viscosity, and $A: B = \text{trace}(AB^T)$ for all square matrices A and B. Including also variations on the boundary $\partial\Sigma$, the first variation of $\mathscr{P}$ reads

$$\delta\mathscr{P}(p, \mathbf{v}; \delta p, \delta \mathbf{v}) = \iint_\Sigma (\delta \mathbf{v} \cdot (-\text{div}_x \mu(\nabla_x \mathbf{v} + \nabla_x \mathbf{v}^T) + \nabla_x p) - \delta p \, \text{div}_x \mathbf{v}) \, dx$$

$$+ \int_{\partial\Sigma} \delta \mathbf{v} \cdot (\mu(\nabla_x \mathbf{v} + \nabla_x \mathbf{v}^T) - pI)\mathbf{n} \, ds.$$

Hence, the requirement that the first variation of $\mathscr{P}$ vanishes for arbitrary variations of v provides the well-known Stokes equations that govern the motion of the fluid under the assumption that the viscous forces are dominant. Moreover, variations with respect to p lead to the equation of continuity. Stated differently, the pressure p can be seen as a Lagrange multiplier which is introduced to take account for the

incompressibility constraint. Finally, it is to be observed that if the equilibrium in the interior of Σ is satisfied the first variation becomes

$$\delta\mathscr{P} = \int_{\partial\Sigma} \delta\mathbf{v} \cdot (\mu(\nabla_x\mathbf{v} + \nabla_x\mathbf{v}^T) - pI)\mathbf{n} \, ds,$$

and $(\mu(\nabla_x\mathbf{v} + \nabla_x\mathbf{v}^T) - pI)\mathbf{n} \, ds$ is the force on a part ds of $\partial\Sigma$.

The Deformation of the Elastic Cylinder

The motion of an elastic particle ξ in the cross section Ω_0 of the undeformed cylinder is a result of both the rigid rotation of the cylinder, $\xi \to \mathbf{X} = R(t)\xi$, and the elastic deformation $\mathbf{X} \to \psi(\mathbf{X})$. Hence, it is natural to describe the mapping of ξ by the combination

$$\xi \to \psi \circ R(t)\xi, \qquad \text{where} \quad R(t) = \begin{bmatrix} \cos\omega t & \sin\omega t \\ -\sin\omega t & \cos\omega t \end{bmatrix}$$

and ω denotes the angular velocity in Ω_0.

The shape of the deformed configuration Ω is constant in time if ψ does not depend on t. The latter will be adopted here and is referred to as *stationary* deformation. However, it is to be stressed that the mapping of the labels depends on time due to the presence of the rotation R. This rotation induces a kinetic energy

$$\iint_\Omega \frac{1}{2}\rho\mathbf{v}^2 \, d\mathbf{x} = \iint_{\Omega_0} \frac{1}{2}\rho_0((\mathbf{v}_\omega \cdot \nabla_\mathbf{X})\psi)^2 \, d\mathbf{X},$$

where ρ denotes the mass density in Ω, ρ_0 the mass density in Ω_0, and $\mathbf{v}_\omega$ is the velocity of the rotation. As is common in the linear theory of elasticity (see, e.g., Marsden and Hughes [9]), the time-independent deformation ψ in the interior of Ω_0 is required to be a stationary point of the Lagrangian

$$\mathscr{E}(\psi) = \frac{1}{2}\iint_{\Omega_0} (C\nabla_\mathbf{X}\psi : \nabla_\mathbf{X}\psi - \rho_0((\mathbf{v}_\omega \cdot \nabla_\mathbf{X})\psi)^2) \, d\mathbf{X}, \tag{2}$$

where C is the elasticity tensor. Or written explicitly, ψ is such that the first variation,

$$\delta\mathscr{E}(\psi; \delta\psi) = \iint_{\Omega_0} (\delta\psi \cdot (-\text{div}_\mathbf{X} C\nabla_\mathbf{X}\psi + \rho_0(\mathbf{v}_\omega \cdot \nabla_\mathbf{X})^2 \psi) \, d\mathbf{X}$$

$$+ \int_{\partial\Omega_0} \delta\psi \cdot C\nabla_\mathbf{X}\psi\mathbf{n}_0 \, ds_0,$$

vanishes for all functions $\delta\psi$.

The Dynamic Variation Principle

Concluding so far, the deformation of the cylinder and the creeping flow of the lubricant are governed by two, different variational principles. In essence, the unified formulation consists of these two constituents plus the requirement that the forces on the common, free boundary

$$\Gamma = \Sigma \cap \Omega$$

should be in equlibrium, i.e.,

$$C \, \nabla_X \psi \mathbf{n}_0 \, ds_0 \circ \psi^{-1} = -(\mu(\nabla_x \mathbf{v} + \nabla_x \mathbf{v}^T) - pI)\mathbf{n} \, ds \qquad \text{on} \quad \Gamma. \tag{3}$$

It is to be noted that the minus sign in this expression is caused by the fact that the normals $\psi(\mathbf{n}_0)$ and $\mathbf{n}$ are opposite: $\mathbf{n}_0$ is the unit outward normal of Ω_0 and $\mathbf{n}$ the unit normal of Σ.

Since the forces in the balance on Γ appeared as boundary terms in the first variations of $\mathscr{E}$ and $\mathscr{P}$, the equations in the interior of the elastic medium and in the fluid as well as the correct balance of force on the common boundary Γ are obtained from

$$\delta\mathscr{P}(p, \mathbf{v}; \delta p, \delta \mathbf{v}) + \delta\mathscr{E}(\psi; \delta \psi) = 0 \tag{4}$$

for all variations subject to

$$\delta \mathbf{v} = \delta \psi \circ \psi^{-1} \qquad \text{on} \quad \Gamma. \tag{5}$$

The free boundary Γ itself is determined by the (no-slip) condition

$$\mathbf{v} = \partial_t(\psi \circ R) \circ (\psi \circ R)^{-1} \qquad \text{on} \quad \Gamma. \tag{6}$$

In addition, the formulation is completed by imposing Dirichlet conditions on the fixed boundaries.

The sound physical foundations of $\delta\mathscr{E} = 0$ and $\delta\mathscr{P} = 0$ seem to be lost in the coupling. In particular, the two terms in (4) differ by a factor with the physical dimension time and the same is true for expression (5). In fact, the mappings ϕ and $\psi \circ R$ (Eq. (6)), as well as the variations of ψ and $\mathbf{v}$ (Eq. (5)), are required to be equal on Γ. However, variations of ψ and $\mathbf{v}$ are in essence very different. Arbitrary, instantaneous variations of the velocity in the fluid can only be achieved by considering time-dependent variations of the mapping of the fluid particles. The elastic deformation ψ is, by contrast, not a function of time. This discrepancy feeds the conception that variations should not be interpreted as being instantaneous, but as continuous *dynamic* changes.

To that end, the δ-operator is viewed as a differentiation with respect to t at a fixed time, say $t = t_0$:

$$\delta = d_t|_{t = t_0}.$$

A variation of the velocity **v** in Σ can then be seen as a change in time

$$\mathbf{V}(\mathbf{x}, t) = \mathbf{v}(\mathbf{x}) + (t - t_0)\, \delta \mathbf{v}(\mathbf{x}),$$

and likewise

$$P(\mathbf{x}, t) = p(\mathbf{x}) + (t - t_0)\, \delta p(\mathbf{x}).$$

Both the elastic deformation ψ itself and variations of ψ do not depend explicitly on time. Therefore, a time-dependent elastic deformation $\boldsymbol{\Psi}(\mathbf{X}, t)$ is to be introduced according to

$$\boldsymbol{\Psi}(\mathbf{X}, t) = \boldsymbol{\psi}(\mathbf{X}) + \tfrac{1}{2}(t - t_0)^2\, \delta \boldsymbol{\psi}(\mathbf{X}).$$

Then, expression (4) can be given the formulation

$$d_t(\mathscr{P}(P, \mathbf{V}) + d_t \mathscr{E}(\boldsymbol{\Psi}))|_{t = t_0} = 0. \tag{7}$$

The constraint (5) and the no-slip condition (6) follow from the requirement that

$$\mathbf{V} = \partial_t(\boldsymbol{\Psi} \circ R) \circ (\boldsymbol{\Psi} \circ R)^{-1} \tag{8}$$

for t in a neighborhood of $t = t_0$. Indeed, putting $t = t_0$ leads to (6) and differentiating (8) with respect to t, holding **x** fixed and taking $t = t_0$, gives the constraint (5).

This provides the observation (4)–(5) of the following *explanation*: the state of the lubricated system will be such that dynamic changes of the velocity and pressure in Σ and the deformation of Ω_0 do (in first order) not alter the total *power* $\mathscr{P} + d_t \mathscr{E}$, where on the common boundary Γ the *no-slip condition* (8) should be satisfied.

The Reynolds–Hertz Approximation

In practice, the task to solve this lubrication problem is relieved by simplifying the formulation. The simplification is based on the assumption that $\varepsilon \ll 1$, where ε is defined as the quotient of the characteristic height and length of Σ (cf. [10]). Formally, both the extremizing velocity and deformation can be calculated as functions of the pressure. If the assumption on the scales of Σ is invoked, that is, if terms of the order ε and higher are neglected, the extremizing velocity in Σ and the extremizing deformation of Ω_0 can actually be calculated, and an integration over the height of Σ can be performed in (7). In doing so, there results (see [8])

$$d_t \int_a^B \left[\frac{H^3}{12\mu} (\partial_x P)^2 - (v_0 + v_k) H\, \partial_x P - \frac{\mu}{H} (v_0 - v_k)^2 \right] dx \Bigg|_{t = t_0} = 0, \tag{9}$$

where the film thickness $H(x, t)$ is given by

$$H(t = t_0) = y_0 - k_0 - \frac{\beta r^2}{k_0} + \gamma \mathscr{L}(p) \quad \text{and} \quad \partial_t H(t = t_0) = 0, \quad (10)$$

and at $t = t_0$, $P(a, t) = P(B, t) = 0$, $P(x, t) > 0$ for $a < x < B(t)$.

Here, the following *notations* are introduced. The constant y_0 denotes the distance between the centre of the cylinder and the rigid surface, and k_0 describes the shape of the undeformed cylinder, i.e., $k_0(x) = \sqrt{(r^2 - x^2)}$, where r is the radius of Ω_0. The x-components of the velocity of the rigid surface and $\mathbf{v}_\omega$ are given by v_0 and v_k, respectively. The constants β and γ depend on the elastic material and the linear operator $\gamma \mathscr{L}(p)$ represents the deflection of the cylinder due to the pressure p. As usual in contact mechanics (cf. [11]), the integral operator $\mathscr{L}$ is approximated by

$$\mathscr{L}(p)(x) = \int_a^b \log |x - s| \, p(s) \, ds. \quad (11)$$

The Inlet and Outlet Boundaries

Finally, it is to be emphasized that the pressure is independent of the height in the considered approximation. This implies that the domain Σ can be described by two x-bounds, a and b. As is usual in EHL theory, the inlet position $x = a$ is fixed while the outlet $x = B(t)$, with $B(t_0) = b$, is treated as a free boundary. By fixing the inlet the total mass flux is, in an implicit way, prescribed. In practice the supply of lubricant is abundant and the mass flux is unknown. This implies that the inlet position has to be chosen far out of the Hertzian (dry) contact region. Later on, numerical experiments will confirm that the precise position of the inlet is than of little importance.

3. THE DISCRETIZATION OF THE TIME VARIABLE

In the light of the dynamic variation principle (7)–(8) an *iteration* for solving the EHL line contact problem is seen as a process which *takes place in time*. That is, with τ an arbitrary, positive time-step, the identifications

$$p^{(i)}(x) = P(x, i\tau), \quad \mathbf{v}^{(i)}(x) = \mathbf{V}(x, i\tau), \quad \mathbf{\psi}^{(i)}(X) = \mathbf{\Psi}(X, i\tau),$$

are made. In this manner the motion of the fluid and the deformation of the elastic medium are characterized by the requirement that the first variation of the total, *time-discrete power*

$$\mathscr{P}(P(i\tau), \mathbf{V}(i\tau)) + \frac{\mathscr{E}(\mathbf{\Psi}(i\tau)) - \mathscr{E}(\mathbf{\Psi}((i-1)\tau))}{\tau}, \quad (12)$$

vanishes for arbitrary variations of the pressure and the velocity in Σ and for arbitrary variations of the deformation of Ω_0 *at time* $t = i\tau$ that satisfy:

$$\delta \mathbf{V}(i\tau) = \frac{\delta \boldsymbol{\Psi}}{\tau} \circ \boldsymbol{\Psi}^{-1}(i\tau) \qquad \text{on} \quad \Gamma. \tag{13}$$

On a superficial view, the principle (12)–(13) is nothing but a reformulation of the observation (4)–(5), where both the functional $\mathscr{E}$ and the variation $\delta \psi$ are divided by τ. Besides, the time-discrete formulation is dressed up by adding a term, namely the functional $\mathscr{E}$ at the time-level $(i - 1)\tau$, which is not part of the variations.

A closer inspection shows that all the salient features of the dynamic variation principle (7)–(8) governing the contact between a fluid and an elastic medium recur in the time discrete formulation. Except one: the (prescribed) time dependence of the elastic deformation differs. This point stands out if one considers variations on and of the common boundary Γ. Here, *the position of Γ can be varied too*, since the fluid domain Σ ($t = i\tau$) depends on the elastic deformation $\boldsymbol{\Psi}(i\tau)$ of the boundary $\partial \Omega_0$. If variations of Σ, due to variations of $\boldsymbol{\Psi}(i\tau)$ on $\partial \Omega_0$ are considered, the boundary term in the first variation of the power functional (12) becomes

$$\left. \int_\Gamma \delta \mathbf{V} \cdot (P - \mu(\nabla \mathbf{V} + \nabla \mathbf{V}^*)) \mathbf{N} \, dx \right|_{t = i\tau} - \frac{1}{\tau} \left. \int_{\partial \Omega_0} \delta \boldsymbol{\Psi} \cdot C \, \nabla \boldsymbol{\Psi} \mathbf{n}_0 \, ds_0 \right|_{t = i\tau}$$

$$+ \left. \int_\Gamma \tau \left(\frac{1}{2} \nabla \mathbf{V} : (\nabla \mathbf{V} + \nabla \mathbf{V}^*) - P \operatorname{div} \mathbf{V} \right) \left(\frac{1}{\tau} \delta \boldsymbol{\Psi} \cdot \mathbf{n}_0 \right) \circ \boldsymbol{\Psi}^{-1} \, ds \right|_{t = i\tau}.$$

The last term in this expression is a result of variations of the fluid domain Σ. The correct equilibrium of forces on Γ (3) is obtained, as before, if the contribution of the variations of Γ to the Euler–Lagrange equation can be neglected. That is, if

$$\tau \, |\nabla \mathbf{V}| \ll 1. \tag{14}$$

Then, the *Euler–Lagrange equations are not altered by taking arbitrary variations of the fluid domain Σ* into account and, consequently, the iterative procedure need not meet the requirement (10): $\partial_t H = 0$.

It goes without saying that the usual simplifications are also performed in the discrete-time formulation. By performing the approximations directly in the variational principle (12)–(13), it can be shown [12] that the evoluation from one time-level to another is governed by the following functional of $P(i\tau)$ and $B(i\tau)$:

$$\int_a^B \left[\frac{H^3}{12\mu} (\partial_x P)^2 - (v_0 + v_k) H \, \partial_k P - \frac{\mu}{H} (v_0 - v_k)^2 \right.$$

$$\left. + \frac{\gamma}{\tau} (P - P((i - 1)\tau) \, \mathscr{L}(P - P((i - 1)\tau)) \right] dx. \tag{15}$$

Arbitrary variations of the simplified power fucntional (15) with respect to the pressure at time $t = i\tau$ lead to

$$\partial_x \left[\frac{-H^3}{12\mu} \partial_x P + \frac{1}{2}(v_0 + v_k)H \right] + \gamma \frac{\mathscr{L}(P) - \mathscr{L}(P((i-1)\tau))}{\tau}$$

$$= \frac{\gamma}{2} \mathscr{L}^* \left[\frac{-H^2}{4\mu}(\partial_x P)^2 + (v_0 + v_k)H \partial_x P - \mu((v_0 - v_k)/H)^2 \right] \quad \text{at } t = i\tau. \tag{16}$$

Moreover, arbitrary variations of the position of the free, outlet boundary $B(i\tau)$ lead to the well-known Swift-Sommerfield, or sometimes also called Reynolds', cavitation condition (cf. [10]),

$$\partial_x P(B(i\tau), i\tau) = 0. \tag{17}$$

The right-hand side of Eq. (16) can be interpreted to result from variations with respect to the film thickness following variations of the pressure. Assuming that inequality (14) is satisfied, the influence of variations of the fluid domain Σ on the Euler–Lagrange equation is nil. This statement is also relevant to the approximation under consideration, since the functional (15) is obtained by substituting the approximating, extremizing velocity $V(i\tau)$ and displacement $\Psi(i\tau)$ into the basic formulation given by Eqs. (12) and (13). This argument justifies the conclusion that the right-hand side of (16) can be neglected. Then, the Euler–Lagrange equation (16) is the well-known *Reynolds equation.*

Physical Interpretation

The pressure is interpreted as a Lagrange multiplier which is introduced to account for the continuity equation. The simplifications leave this view undisturbed: the Euler–Lagrange equation (16) is a discretization of the *integrated balance of mass.* To illuminate this assertion the time-discrete mass flux

$$M_f^{(i)} = \int_k^{y_0} V_1 \, dy \big|_{t = i\tau} \tag{18}$$

is introduced. Since the mass density ρ of the lubricant is assumed to be constant, the integrated balance of mass can be expressed in terms of the flux M_f and the time rate change of the film thickness h:

$$0 = \frac{M_f^{(i)}(x + \Delta) - M_f^{(i)}(x)}{\Delta} + \int_x^{x + \Delta} \mathbf{V} \cdot \mathbf{N} \big|_{y = k, t = i\tau} \, ds$$

$$\stackrel{(\Delta \to 0)}{=} \partial_x M_f^{(i)} + \frac{h^{(i)} - h^{(i-1)}}{\tau}. \tag{19}$$

The equivalence of the Euler–Lagrange equation (16), with right-hand side equal to zero, and the balance of mass (19) is establishes by substituting the extremizing

velocity field (which is a Poiseuille–Couette flow; see, e.g., [10]) into (19). The substitution gives [10]

$$M_f^{(i)} = -\left(\frac{h^{(i)}}{12\mu}\right)^3 \partial_x p^{(i)} + \frac{1}{2}(v_0 + v_k)h^{(i)}. \tag{20}$$

Concluding, the dynamic iteration follows the *physical evolution of the balance of mass*. In this respect the present approach differs from the iterative methods as mentioned in Section 1. The need to have a constant mass flux through the contact is a physical necessity, which is met here. On the contrary, as is reported by Goglia [13], as well as by others, the Gauss–Seidel iterative methods can lead to mass flux defects up to 20%.

The governing power functional (15) is not quadratic in terms of the pressure. This implies that several additional iterations within every time step are necessary as an aid in calculating the extremizing pressure distribution $p^{(i)}$. In a classical approach, the resulting non-linear Euler–Lagrange equation would be solved using a Newton–Raphson iteration (see, e.g., [14]). However, the observation that variations of Σ are of secondary importance indicates another way out: *the fluid domain Σ is frozen in*. This strategy gives the following iterative procedure.

THE ITERATION SCHEME. The iterates $p^{(i)}$, $i = 1, 2, 3, ...$, with $p^{(i)} > 0$ on $(a, b^{(i)})$ and $p^{(i)} = 0$ elsewhere, minimize

$$\int_a^b \left[\frac{h^3}{12\mu}(d_x p)^2 - (v_0 + v_k)h\, d_x p - \frac{\mu}{h}(v_0 - v_k)^2 \right.$$
$$\left. + \frac{\gamma}{\tau}(p - p^{(i-1)})\,\mathscr{L}(p - p^{(i-1)}) \right] dx, \tag{21}$$

where the film thickness is evaluated at the old time level

$$h = y_0 - k_0 - \frac{\beta r^2}{k_0} + \gamma \mathscr{L}(p^{(i-1)}), \tag{22}$$

and $p^{(0)} = $ given. Moreover, arbitrary variations of (21) with respect to the position of the cavitation boundary b lead to the free boundary condition (17).

Evaluating the film thickness at time $t = (i-1)\tau$ introduces an error in the Euler–Lagrange equation. The Euler–Lagrange equation resulting from arbitrary variations of (21) with respect to $p^{(i)}$ is

$$\partial_x \tilde{M}_f^{(i)} + \frac{h^{(i)} - h^{(i-1)}}{\tau} = 0, \tag{23}$$

where

$$\tilde{M}_f^{(i)} = -\frac{(h^{(i-1)})^3}{12\mu} \partial_x p^{(i)} + \frac{1}{2}(v_0 + v_k)h^{(i-1)}.$$

The linear Euler–Lagrange equation (23) differs from (20). By introducing a Taylor expansion of the film thickness $h^{(i)}$ the dissimilarity can be stated explicitly: a solution of (23) satisfies

$$\partial_x M_f^{(i)} = \partial_x \tilde{M}_f^{(i)} + 3\tau\,\partial_x \left[\left[\frac{M_f^{(i)}}{h^{(i-1)}} - \frac{v_0 + v_k}{2} \right] \partial_t h \right] + \mathcal{O}(\tau^2).$$

The time-step τ is assumed to be so small that the terms of the order τ^2 and higher can be neglected. Then, Eq. (23) forms a good approximation of (20) if

$$3\tau\,|\partial_x| \left| \frac{M_f^{(i)}}{h^{(i-1)}} - \frac{v_0 + v_k}{2} \right| \ll 1. \tag{24}$$

In terms of a characteristic velocity $\mathbf{v}$ in x-direction and a characteristic height $\mathbf{h}$ (y-direction) of the fluid domain Σ the flux M_f can be scaled by $\mathbf{vh}$. This shows that the requirement (24) is fulfilled if the time step τ satisfies

$$\tau \mathbf{v} \ll \mathbf{1}, \tag{25}$$

where $\mathbf{1}$ is a characteristic length (x-direction) of Σ.

This constraint provides the linear iteration scheme (21)–(22) of a sound basis. The film thickness can be evaluated on a preceding time level if the time step is restricted to (25). The non-linear formulation (15) itself is an approximation. Thus, from a theoretical point of view, the linearization given by (21)–(22) can be called exact if $\tau \mathbf{v} = \mathcal{O}(\varepsilon)\mathbf{1}$. It may be observed that this requirement is identical to (14), since $|\nabla \mathbf{v}| = \mathcal{O}(\mathbf{v}/\mathbf{h})$.

Physically, the requirement (25) expresses that the time-step should be much smaller than the residence time $\mathbf{1}/\mathbf{v}$ in which a fluid particle moves through the domain Σ. In this light the restriction (25) seems to be mild. The more so, since the need to linearize (15) is a necessity for computing a steady state solution p of this non-linear EHL problem.

4. THE DISCRETIZATION OF THE SPACE VARIABLE

Up to this point, the mathematical model has been approximated in such a way that the variational structure is maintained. Our next aim is to solve the resulting discrete-time problem. The underlying structure dictates the way to proceed: the iteration scheme (21)–(22) has to be executed. To that end the continuous pressure function $p^{(i)}$ on $[a, b]$ is discretized by restricting it to a finite dimensional space.

The x-domain is extended to $[a, b_0]$ with $b_0 > b^{(i)}$ ($i = 1, 2, 3, ...$) and the pressure $p^{(i)}$ is restricted to positive values for $a < x < b^{(i)}$ and equal to zero otherwise. The *projection* into a finite dimensional space can then be written as

$$p^{(i)}(x) = \sum_{j=0}^{N+1} p_j^i T_j(x) \qquad \text{for} \quad a \leqslant x \leqslant b_0. \tag{26}$$

The basis functions T_j are chosen as

$$T_j(x) = \begin{cases} (x - x_{j-1})/\Delta_j & \text{if} \quad x_{j-1} < x < x_j \ (j \neq 0) \\ 0 & \text{if} \quad x < x_{j-1} \ \text{or} \ x > x_{j+1} \\ (x_{j+1} - x)/\Delta_{j+1} & \text{if} \quad x_j < x < x_{j+1} \ (j \neq N+1), \end{cases}$$

where the grid points x_j satisfy

$$a = x_0 < x_1 < \cdots < x_j < x_{j+1} < \cdots < x_{N+1} = b_0, \qquad \Delta_j = x_j - x_{j-1}.$$

These points are not necessarily uniformly distributed over the interval $[a, b_0]$. The tent functions T_j are non-negative, have local support and further, $T_j(x_k) = 1$, if $k = j$, and $= 0$ otherwise. Owing to these properties the non-negativity constraint on the pressure translates into a non-negativity constraint on the coefficients:

$$p_j^i \geqslant 0 \qquad (\text{for} \ j = 1, 2, ..., N). \tag{27}$$

Moreover, the boundary conditions are satisfied by taking $p_0^i = p_{N+1}^i = 0$.

A numerical solution characterized by the non-negative coefficients

$$\mathbf{p}^i = (p_1^i, p_2^i, ..., p_N^i)$$

minimizes the time-discretized functional (21). The constraint (27) is satisfied by setting p_j^i (for $j = k, k+1, ..., N$) equal to zero, whenever the kth component of the solution is negative. In this formalism, the free boundary $b^{(i)}$ is just the first point to the right of a, where $p^{(i)} = 0$. Such a solution is solely acceptable if $p_N^i = 0$. Otherwise, the boundary $x = b_0$ is not chosen properly, and the domain has to be enlarged in such a way that the relation $b_0 > b^{(i)}$ holds.

The functional (21) can be expressed in terms of the coefficients $\mathbf{p}^i$. Dropping two unessential constants in (21), namely,

$$\int_a^b \mu(v_0 - v_k)^2/h \, dx \qquad \text{and} \qquad \int_a^b p^{(i-1)} \mathcal{L}(p^{(i-1)}) \, dx,$$

the discretization can be given as follows:

The vector $\mathbf{p}^i > 0$ minimizes

$$A\mathbf{p} \cdot \mathbf{p} - \mathbf{f} \cdot \mathbf{p} + \frac{\gamma}{\tau}(\mathbf{p} \cdot \bar{L}\mathbf{p} - 2\mathbf{p} \cdot \bar{L}\mathbf{p}^{i-1}), \tag{28}$$

where the tridiagonal $N \times N$-matrix A is given by

$$A_{jj} = a_j + a_{j+1}, \qquad A_{jj+1} = A_{j+1j} = -a_{j+1}, \qquad A_{jk} = 0 \qquad \text{for} \quad k \neq j-1, j, j+1$$

with

$$a_j = \int_{x_{j-1}}^{x_j} \frac{h^3}{12\mu} \frac{dx}{(\Delta_j)^2}.$$

Further, the components of the N-vector $\mathbf{f}$ are

$$f_j = \int_{x_{j-1}}^{x_j} (v_0 + v_k) h \frac{dx}{\Delta_j} - \int_{x_j}^{x_{j+1}} (v_0 + v_k) h \frac{dx}{\Delta_{j+1}}$$

and the elements of the $N \times N$-matrix $\bar{L}$ are defined by

$$\bar{L}_{jk} = \int_{x_{j-1}}^{x_{j+1}} T_k \mathscr{L}(T_j)\, dx,$$

where

$$\mathscr{L}(T_j) = \frac{(x - x_{j-1})^2}{2\Delta_j} \log |x - x_{j-1}| + \frac{(x - x_{j+1})^2}{2\Delta_{j+1}} \log |x - x_{j-1}| - \frac{3}{4} (\Delta_j + \Delta_{j+1})$$

$$- \frac{1}{2} \left[\frac{1}{\Delta_j} + \frac{1}{\Delta_{j+1}} \right] (x - x_j)^2 \log |x - x_j|.$$

In principle the integral expressions for a_j, f_j, and $\bar{L}_{jk}$ can be calculated analytically. However, the numerical evaluation of the analytical expressions requires quite an effort, due to their complexity. For this reason the integrals a_j, f_j, and $\bar{L}_{jk}$ are approximated by the trapezoidal rule. In doing so, the integrals adopt the simple forms

$$a_j = \frac{1}{24\Delta_j} \left[h^3(x_j) + h^3(x_{j-1}) \right]$$

$$f_j = \tfrac{1}{2} \left[(v_0 + v_k) h(x_{j-1}) - (v_0 + v_k) h(x_{j+1}) \right]$$

$$\bar{L}_{jk} = \tfrac{1}{2} (\Delta_j + \Delta_{j+1}) \mathscr{L}(T_k(x_j)).$$

The symmetrical, tridiagonal matrix A is diagonally dominant and positive definite, while the elements of $\bar{L}$ are all strictly negative.

5. The Iterative Procedure

Naturally, the dynamic procedure for the EHL problem consists of step by step proceeding in time. Two aspects of this time-like route deserve careful attention. First, the path towards the steady-state solution can be cut off by controlling the physical parameter γ. Second, and much more important, the distance between the centre of the cylinder and the rigid surface, i.e., y_0, is not given in advance. Instead, the loading F on the cylinder is prescribed. This force should be balanced by the (pressure) forces on Γ:

$$F = \int_a^b p(x)\, dx. \tag{29}$$

This setting of the problem can be built into the iterative procedure.

Continuation of the Parameter γ

Returning to the role of the parameter γ it is to be noted that the lubrication problem becomes linear if $\gamma = 0$. Or in different words, γ measures the influence of the non-linear term and by that also the number of iterations. Therefore the iteration is started with $\gamma = 0$, whereupon this parameter is decreased by $\Delta\gamma$ at every time-step until the desired, final (negative) value is reached. Physically, this process corresponds to an initially rigid cylinder which is weakened in the course of time. By choosing an adequate subdivision, the continuation process converges faster then the straightforward calculation starting with the prescribed value of γ. An example which confirms this assertion is given in Fig. 2.

Satisfying the Load Equation (29)

As remarked above the iteration has to be adapted if the loading F, and not the distance y_0, is given in advance. It is important to realize that in engineering practice the loading is so high that the distance between the centre of the deformed cylinder and the rigid surface is smaller than the radius of the cylinder: $y_0 < r$. Therefore, the distance y_0 is considered as a function of the time, y_0^i, and is changed in time in such a way that the integral over $p^{(i)}$ converges to F, while the film thickness is strictly positive. So, starting from a value greater than the radius of the
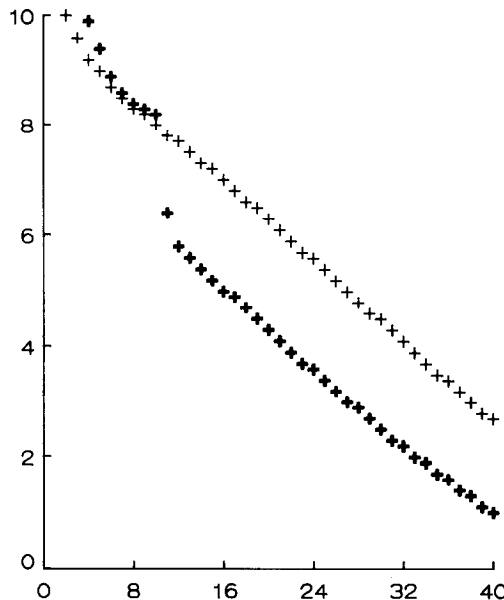

FIG. 2. The convergence with and without the continuation of the parameter γ: the difference $\log(1 + \max |p^i - p^{i-1}|)$ versus i. The stiffness of the cylinder is slowly decreased according to $\gamma^i = i\,\Delta\gamma$ for $i = 1, ..., 10$ and constant for $i > 10$ (bold crosses) or constant for all i, i.e., $\gamma^i = 10\Delta\gamma$ for $i > 0$ (crosses). $\Delta\gamma = 1.2 \times 10^{-8}$, the Moes number $M \simeq 0.9$ (i.e., $y_0^i \simeq r$), and $\Delta t = 5 \times 10^{-5}$.

cylinder, y_0 is reduced per time step. This reduction, limited by the requirement that the film thickness should be positive, induces a constant velocity $(y_0^i - y_0^{i-1})/\tau$ perpendicular to the rigid surface. This contributes to the time-rate change of the film thickness and has to be included in the functional (28). Then the governing functional (28) changes into

$$A\mathbf{p} \cdot \mathbf{p} - \mathbf{\tilde{f}} \cdot \mathbf{p} + \frac{\gamma}{\tau}(\mathbf{p} \cdot \bar{L}\mathbf{p} - 2\mathbf{p} \cdot \bar{L}\mathbf{p}^{i-1}), \tag{30}$$

where

$$\tilde{f}_j = f_j - \frac{1}{2\tau}(\varDelta_j + \varDelta_{j+1})(y_0^i - y_0^{i-1}).$$

Figure 3 shows a typical development of the iteration. The increase of the load lags after the reduction of the distance y_0. And the magnitude of the maximum difference between subsequent iterates is almost constant during this process.

If the physical constraint $h > 0$ is not satisfied, the solution $\mathbf{p}^i$ is rejected, the speed $(y_0^i - y_0^{i-1})/\tau$ is slackened, and $\mathbf{p}^i$ is calculated again. Moreover, if the film thickness is still not strictly positive, the solution $\mathbf{p}^i$ is rejected again and so on. In practice, the speed at which the rigid surface approaches the cylinder can be
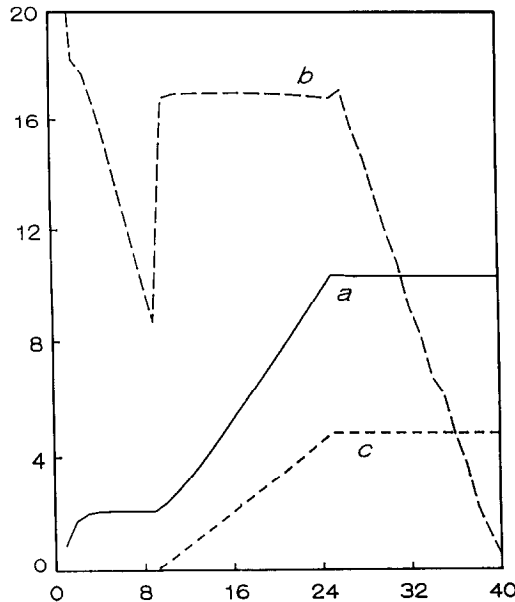

Fig. 3. The increment of the load and the difference between subsequent iterates resulting from a reduction of the distance y_0. The load $\int p^i$ (graph a), the difference $\log(1 + \max |p^i - p^{i-1}|)$ (b, dashed) and the distance $r - y_0^i$ (c, dashed) versus i for $i = 1, 2, ..., 40$. The integral over p^i and the difference $r - y_0^i$ are multiplied by $1E{-}4$ and $1E6$, respectively, $M \simeq 5$, $N = 80$, $\varDelta t = 10^{-5}$.

kept constant over a large number of iterations, and a calculated solution $\mathbf{p}^i$ is rejected rarely.

The decrease of y_0 is stopped when the integral over the pressure is close to the load F and the steady state belonging to y_0, denoted by $p(x; y_0)$, is calculated. Then, Eq. (29) is satisfied by an iterative procedure. That is, y_0 is increased if $\int_a^b p(x; y) \, dx > F$ and decreased if otherwise, and the steady state solution belonging to the new value of y_0 is calculated. If necessary y_0 is adjusted again, and the procedure is repeated.

Summarizing, the *algorithm* reads

initial
$$i := 0, \ p^i := 0, \ \bar{\gamma} := 0, \ y_0 := r + \delta.$$

time-step
1. $h^i := y_0 - k_0 - (\beta r^2 / k_0) + \bar{\gamma} L p^i$
    correction: if $h^i < 0$ then reject and increase y_0; iteration.
2. solve p^{i+1} from Eq. (30)
    cavitation: if $p_i^{i+1} \leqslant 0$ then $p_k^{i+1} := 0$ for $k = i, i+1, ..., N$
    correction (domain): if $b^{i+1} = b_0$ or $b^{i+1} \ll b_0$
    $\qquad\qquad\qquad\qquad$ then adjust b_0; iteration.
3. $i := i + 1$.

iteration
in case of
    A. $\bar{\gamma} < \gamma$: $\bar{\gamma} := \bar{\gamma} - \Delta\gamma$, time step.
    B. $\int p^i \, dx - F > \varepsilon_1 > 0$: $y_0 := y_0 + \Delta y_0$, time-step.
    C. $F - \int p^i \, dx > \varepsilon_1 > 0$: $y_0 := y_0 - \Delta y_0$, time-step.
    Otherwise.
        If $\max |(p^i - p^{i-1})/p^i| > \varepsilon_2$ or $|b^i - b^{i-1}| > \varepsilon_3$ then time-step else stop.

Remark. Instead of taking $p = 0$ as an initial state, the iteration can also be started with a solution that is calculated previously.

6. Proceeding in Time by Preconditioning

This section deals with the numerical problem of solving the pressure $\mathbf{p}^i$ from the discretized power (30). The Euler–Lagrange equation resulting fro variations with respect to $\mathbf{p}^i$ is

$$\left(A + \frac{\gamma}{\tau} \bar{L} \right) \mathbf{p}^i = \frac{1}{2} \bar{\mathbf{f}} + \frac{\gamma}{\tau} \bar{L} \mathbf{p}^{i-1} \tag{31}$$

and $\mathbf{p}^i$ has to be solved from this linear system of equations. Solving Eq. (31) at every time step is not very attractive, due to the fact that $\bar{L}$ is a full matrix. This property of $\bar{L}$, in spite of the local support of the basis functions T_i, reflects the global character of the integral operator $\mathscr{L}$.

Reduction to a Quasi-Pentadiagonal System

The matrix $\bar{L}$ will now be considered in more detail. To start, $\bar{L}$ is written as the product of a diagonal matrix D and a matrix L,

$$\bar{L} = DL,$$

defined by

$$D = \tfrac{1}{2} \operatorname{diag}(\varDelta_1 + \varDelta_2, \varDelta_2 + \varDelta_3, ..., \varDelta_N + \varDelta_{N+1}), \qquad L_{jk} = \mathscr{L}(T_k)(x_j).$$

Apart from a multiplicative factor the jth column of the matrix L can be seen as the normal component of the displacement at the boundary of the cylinder caused by a pressure distribution described by the jth basis function T_j. This interpretation feeds the idea that the operator $\mathscr{L}$ maps the local function T_j into a global function. And that, in reverse, the operator $\mathscr{L}^{-1}$ maps an argument with local support into an image with local support. As is shown in Fig. 4, deformation of the contact surface resulting from a localized force $T_{25}(x)$ is indeed global: The displacement at the boundaries of the interval $[a, b]$ resulting from the force $T_{25}(x)$, which is located in the middle of this interval, is approximately one-half of the displacement in the middle.
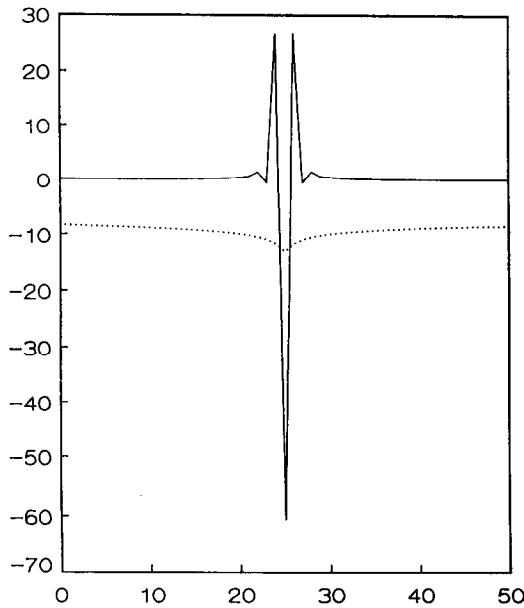

FIG. 4. The discretized deflection operator L and its inverse. The dotted line represents $\mathscr{L}(T_{25})$; the continuous line $\mathscr{L}^{-1}(T_{25})$. By definition, the elements $L_{j,25}$ of the 25th row of the $50 * 50$ matrix L are given by $\mathscr{L}(T_{25})(x_j)$, where $j = 1, 2, 3, ..., N = 50$, and the corresponding elements of the inverse are given by $\mathscr{L}^{-1}(T_{25})(x_j)$. The equidistant grid that is used covers the domain $[-0.0004, 0.0001]$, and the elements $L_{j,25}$ and $L_{j,25}^{-1}$ are multiplied by 10^5 and 10^{-3}, respectively. It is to be observed that the matrix L^{-1} resembles a tridiagonal matrix.

On the other hand, the force needed to obtain a displacement given by $T_{25}(x)$ is self-also-localized. Stated differently, the elements of the inverse L^{-1} are concentrated around the diagonal. Particularly, this last observation motivates us to multiply Eq. (31) by the tridiagonal matrix $\bar{Q}$ that is a truncation of L^{-1}:

$$\bar{Q}_{jk} = L_{jk}^{-1} \quad \text{if} \quad j = k-1, k, k+1, \text{ and } = 0 \text{ otherwise.}$$

Then, the following linear system has to be solved:

$$\left(\bar{Q}D^{-1}A + \frac{\gamma}{\tau}\bar{Q}L \right) \mathbf{p}^i = \frac{1}{2}\bar{Q}D^{-1}\hat{\mathbf{f}} + \frac{\gamma}{\tau}\bar{Q}L\mathbf{p}^{i-1}. \tag{32}$$

The product $\bar{Q}D^{-1}A$ is a pentadiagonal matrix. Thus, the linear system (32) can be approximated by a pentadiagonal system if the product $\bar{Q}L$ resembles a pentadiagonal matrix. However, as it appears from Fig. 5, the product $\bar{Q}L$ cannot be approximated by a pentadiagonal matrix. In fact, $\bar{Q}$ is a poor approximation of the inverse L^{-1}: the difference between $\bar{Q}L$ and the identity is not constant over almost the entire domain, and so much the worse, is large near and at the boundaries.

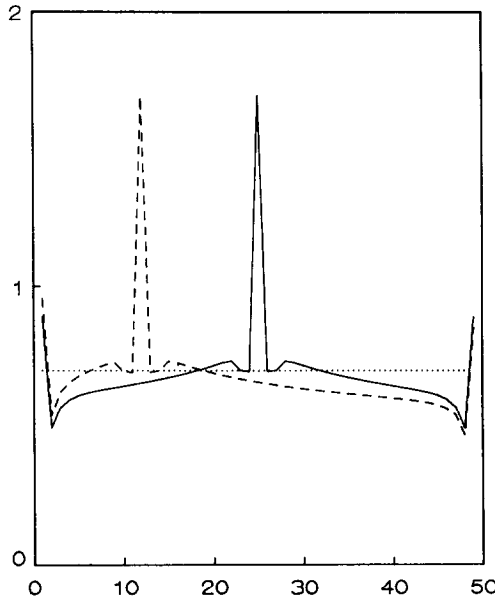Looking at Fig. 4 again, the tridiagonal matrix $\bar{Q}$ is almost a discrete representa-

FIG. 5. The product of L and the approximation of L^{-1} by the tridiagonal matrix $\bar{Q}$. This figure shows two rows of the product $\bar{Q}L$: $\bar{Q}L_{i25}$ and $\bar{Q}L_{i12}$ (dashed), where $i = 1, 2, 3, ..., N = 50$. The tridiagonal matrix $\bar{Q}$ is given by $\bar{Q}_{ij} = L_{ij}^{-1}$ for $|i - j| \leqslant 1$. The grid and domain are the same as in Fig. 4. From this figure it is concluded that $\bar{Q}$ is not well suited as a preconditioner, since multiplying L with $\bar{Q}$ does not lead to a matrix that resembles a band-matrix.

tion of the *second* derivative with respect to x. Almost, since the sum of the row elements of $\bar{Q}$ is not zero. This effect causes dissipation and for this reason a more gross approximation of the inverse is adopted, namely, the discretization of the second derivative. That is, the rows (except the first and the last one) of the preconditioner are modified to

$$[Q_{j-1j}, Q_{jj}, Q_{jj+1}] = C_j \left[\frac{-1}{\varDelta_j(\varDelta_j + \varDelta_{j+1})}, \frac{1}{\varDelta_j \varDelta_{j+1}}, \frac{-1}{\varDelta_{j+1}(\varDelta_j + \varDelta_{j+1})} \right], \quad (33)$$

where the constants C_j are chosen in such a way that the diagonal elements of QL are of the order one. Obviously, there is no need to compute the inverse of L when the preconditioner (33) is used instead of $\bar{Q}$. This preconditioner is satisfactory if the product QL can be approximated by a pentadiagonal (or, more general, by a band-) matrix.

The second derivative of $\mathscr{L}T_j(x)$ can be calculated analytically and reads

$$d^2_{xx} \mathscr{L}(T_j) = \frac{1}{\varDelta_j} \log \left| 1 + \frac{\varDelta_j}{x - x_j} \right| + \frac{1}{\varDelta_{j+1}} \log \left| 1 - \frac{\varDelta_{j+1}}{x - x_j} \right|$$

for $x < x_{j-1}$ and for $x > x_{j+1}$. The Taylor expansion of this expression shows that the second derivative of $\mathscr{L}(T_j)$ behaves (in first order) as

$$d^2_{xx} \mathscr{L}(T_j) = \frac{\varDelta_j + \varDelta_{j+1}}{2(x - x_j)^2}. \quad (34)$$

In conclusion, the second derivative of $\mathscr{L}(T_j)$ decays as $(x - x_j)^{-2}$ for $x < x_{j-1}$ and for $x > x_{j+1}$. This shows that Q is indeed a good candidate for the preconditioner, since the product of Q and $\mathscr{L}(T_j)$ is localized around $x = x_j$. In addition, it is to be remarked that taking higher derivatives of $\mathscr{L}(T_j)$ than the second derivative will lead to a better concentration around $x = x_j$. However, this advantage is outweighed by the fact that the product of the discretization of such a higher derivative and the matrix A contains many more non-zero elements than the product of Q and A.

Further, on the basis of the symmetry $\mathscr{L}(T_j)(x_j - x) = \mathscr{L}(T_j)(x_j + x)$, it is concluded that the boundary conditions belonging to the derivative operator d^2_{xx} are Neumann conditions. However, if the first and last row of Q are taken as

$$Q_{11} = -Q_{12} = \frac{2C_1}{(\varDelta_1 + \varDelta_2)}, \qquad Q_{NN} = -Q_{NN-1} = \frac{2C_N}{(\varDelta_N + \varDelta_{N+1})}, \quad (35)$$

the matrix Q becomes singular. Indeed, the kernel of the second derivative operator with Neumann boundary conditions is spanned by the constant function. Regarding Eq. (31) this implies that the level of

$$\left(D^{-1}A + \frac{\gamma}{\tau} L \right) \mathbf{p}^i - \frac{1}{2} D^{-1}\bar{\mathbf{f}} - \frac{\gamma}{\tau} L \bar{\mathbf{p}}^{i-1}$$

ought to be set equal to zero. This can be achieved by taking

$$Q_{12} = 0 \qquad (36)$$

instead of (35), while Q_{11} is unchanged. The result of this approximation is shown in Fig. 6.

The product QL cannot be approximated by a pentadiagonal matrix, due to the fact that in this approach the weight of the first row is not concentrated around the diagonal. More precisely, the multiplication with Q does not alter the ratio between the elements of the first row of L. Therefore, the product QL is a so-called *quasi-pentadiagonal matrix*, i.e., a pentadiagonal matrix with one full row. In this manner, the global character of the operator $\mathcal{L}$ is still present.

Solving the Quasi-Pentadiagonal System

A quasi-pentadiagonal system can be solved efficiently by a partition method (see, e.g., Fröberg [15]). Denoting the quasi-pentadiagonal matrix (with a full first row) by S and considering the system $S\mathbf{p} = \mathbf{r}$, the first equation is separated from the rest, i.e.,

$$S = \begin{pmatrix} s_{11} & \mathbf{s}^* \\ \boldsymbol{\sigma} & \bar{S} \end{pmatrix}, \qquad \mathbf{p} = \begin{pmatrix} p_1 \\ \bar{\mathbf{p}} \end{pmatrix}, \qquad \mathbf{r} = \begin{pmatrix} r_1 \\ \bar{\mathbf{r}} \end{pmatrix},$$
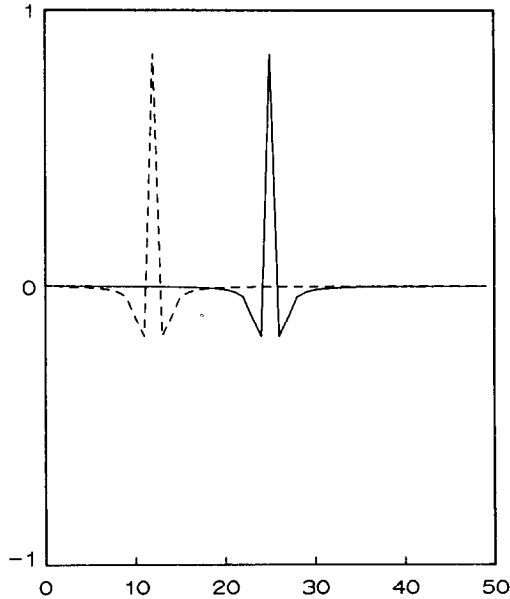

FIG. 6.   The product of L and the preconditioner Q. This figure shows two rows of the product QL: $QL_{i,25}$ and $QL_{i,12}$ (dashed), where $i = 1, 2, 3, ..., N = 50$. The preconditioner Q is given by (33), (35), and (36). The grid and domain are the same as in Fig. 4. Compared to that figure, the multiplication of the matrix L is much more successful; here the product of the matrices can be approximated by a tridiagonal matrix.

with, for j, $k = 1, 2, 3, ..., N - 1$,

$$\bar{S}_{jk} = S_{j+1\,k+1}, \qquad s_j = S_{1\,j+1}, \qquad \sigma_j = S_{j+1\,1}, \qquad \bar{p}_j = p_{j+1}, \qquad \bar{r}_j = r_{j+1}.$$

Then, the solution $(p_1, \bar{\mathbf{p}})$ is given by

$$(s_{11} - (\mathbf{s} \cdot \mathbf{z}))\, p_1 = r_1 - (\boldsymbol{\sigma} - \mathbf{w}), \qquad \bar{\mathbf{p}} = \mathbf{w} - p_1 \mathbf{z}, \qquad \text{where} \quad \bar{S}\mathbf{w} = \bar{\mathbf{r}}, \; \bar{S}\mathbf{z} = \boldsymbol{\sigma}.$$

Hence, the solution $\mathbf{p}$ can be calculated straightforwardly from the vectors $\mathbf{w}$ and $\mathbf{z}$. These two unknowns can be solved easily, since $\bar{S}$ is a pentadiagonal matrix. If this is done by a LU decomposition, the solution of a quasi-pentadiagonal system takes only approximately 50 % more operations $(+, -, *)$ than solving a pentadiagonal system. This difference will even be less in computation time, since additional divisions can be avoided.

7. RESULTS

Recent developments in the field of EHL resulted into an "efficient and robust" solver [16] which runs on a (Cray XMP) supercomputer and a "very powerful" multigrid technique [5] which takes up the storage of a powerful computer. Compared to these algorithms the present approach requires moderate computer facilities. In fact, the dynamic iteration is implemented on a personal computer (Olivetti M240), where the computer run time varies between one and ten minutes.

Considering the dynamic approach in detail there is, of course, no need to calculate the intermediate results with a high accuracy. For this reason the subsequent iterates are calculated on a relatively coarse grid. Then, after the steady state is approached, the solution is interpolated on a finer grid and the iteration is continued until the stopping criterion is satisfied. Figure 7 shows two intermediate results, which are found at approximately one-third and two-thirds of the total number of iterations. These iterates are calculated using only 25 nodes. The final solution is written as a combination of 100 basis functions. As it appears from Fig. 8, the difference between this solution and the steady state calculated with $N = 25$ is small. From an engineering point of view the latter is as satisfactory as the former.

Here, the inlet position $x = a$ is fixed while the outlet $x = b$ is treated as a free boundary. The fixation of the inlet is based on the assumption that its precise position has no (or, better, little) influence on the solution. The present calculations confirm the statement made in [17] that $a = -4b_h$, where b_h denotes the semiwidth of the Hertzian contact, is a good choice for moderate and highly loaded contacts. However, if the contact is lightly loaded, that is if the number

$$M := F(-\pi \gamma / (r\mu(v_0 + v_k)))^{0.5},$$

which is introduced by Moes [18], is smaller than 5, the inlet area should be larger in order to prevent starvation. This effect is illustrated in Fig. 9.
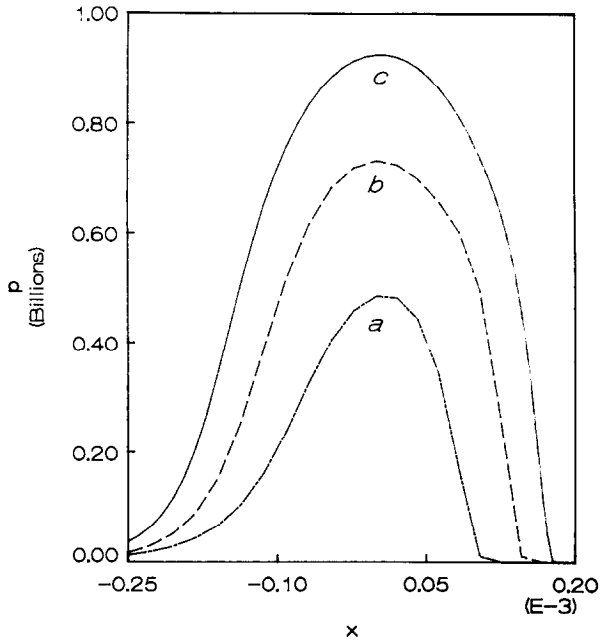
FIG. 7. The steady-state solution and two intermediate results. The pressure $p^i(x; y_0^i)$, where $r - y_0^i$ is two times the steady-state distance $r - y_0$ in graph b and three times that in a. The graphs a and b are calculated with $N = 25$, while the steady state (c) is represented using 100 basis functions. The physical parameters used are (in SI units): $a = -1E - 3$, $\mu = 0.3$, $r = 0.01$, $y_0 = 0.009985$, $\omega = 50$, $v_0 = \omega r = 0.5$, $\rho = 8000$, E (= Young modulus) $= 1E11$, v (= constant of Poisson) $= 0.3$ ($M \simeq 10$).
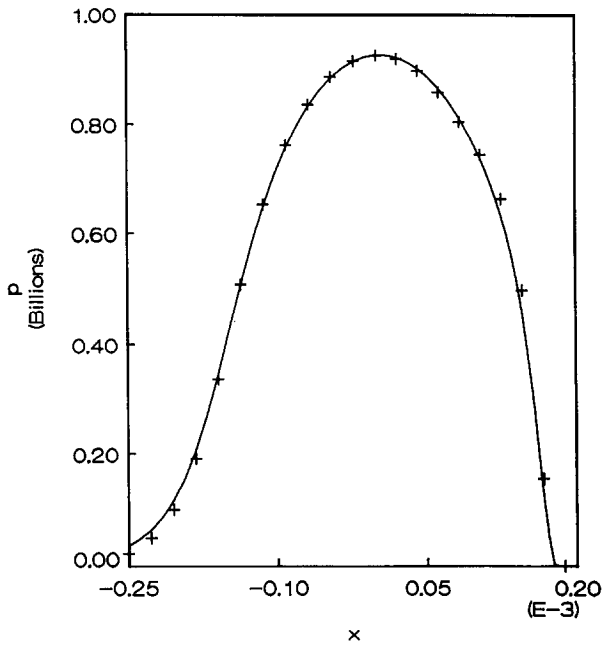
FIG. 8. Dependence of the calculated pressure distribution on the number of gridpoints. The pressure p where the parameters are as in Fig. 7c, with $N = 100$ and $N = 25$ (crosses).

482
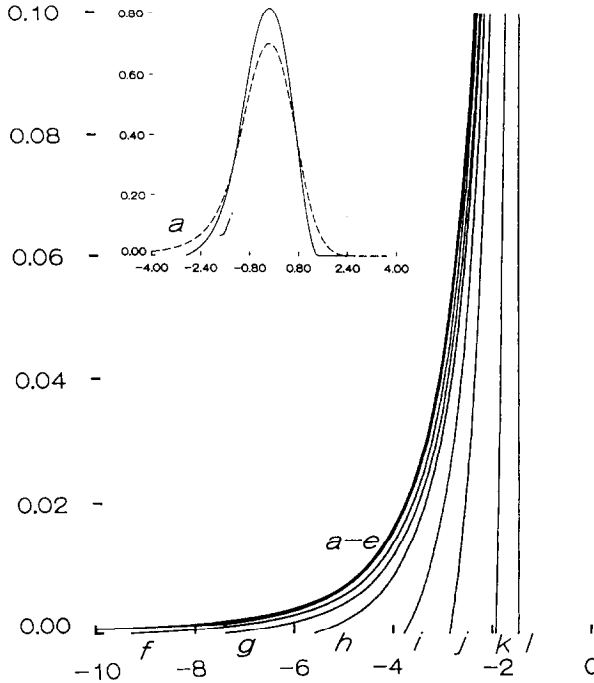
FIG. 9. The dependence on the position of the inlet boundary. The pressure p in the inlet region for differnt choices of the inlet position $x = a$: $a = -1E - 2 = -r$ (a); $-8E - 3$ (b); $-6E - 3$ (c); $-4E - 3$ (d); $-2E - 3$ (e); $-1E - 3$ (f); $-8E - 4$ (g); $-6E - 4$ (h); $-4E - 4$ (i); $-3E - 4$ (j); $-2E - 4$ (k); $-1.5E - 4$ (l). The Moes number $M \simeq 3$, the space variable is scaled on the Hertzian pressure. The inset shows the global pressure distribution in the cases a and j.

Hence, for lightly loaded contacts the inlet region is large compared to the width of the Hertzian contact, while on the other hand the pressure gradients in the inlet are comparatively small. Therefore a non-equidistant grid is used. In this context, it is to be remarked that the mesh sizes should be of the form $\Delta_j = n_j \Delta$ (where n_j is an integer) in order to maintain that part of the symmetry of the matrix L, which allows for a storage of only $\mathcal{O}(N)$ elements.

Pressure distributions and film thicknesses obtained by the dynamic iteration method are given in Fig. 10 and 11, respectively. The parameter setting corresponds to a realistic steel–mineral oil contact. The minimal film thickness are very much in agreement with the formula given in [5]. As can be seen from Fig. 12 the thickness and the free, cavitation boundary. A blowup of the pressure around the cavitation boundary $x = b$ is given in Fig. 13, where a non-equidistant refinement of the grid is used. Clearly, the numerical solution does not satisfy the free boundary condition (17) exactly, but in view of the large gradients involved, the tendency towards (17) is visible.
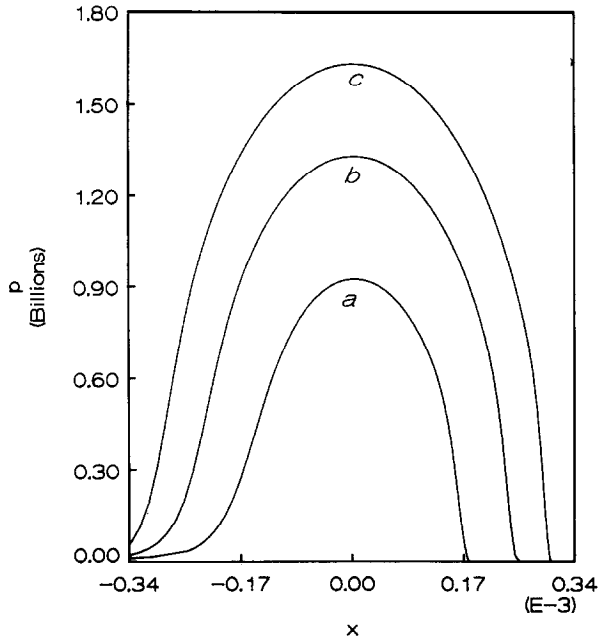
FIG. 10. The dependence of the pressure on the loading. The pressure p for three different values of the loading: $w = 2.57E5$ (a); $5.15E5$ (b); $7.71E5$ (c). The physical parameters are as in Fig. 7, except $a = -1.25e - 3$ and, of course, y_0 differs. The Moes numbers are approximately 10, 20, and 30.
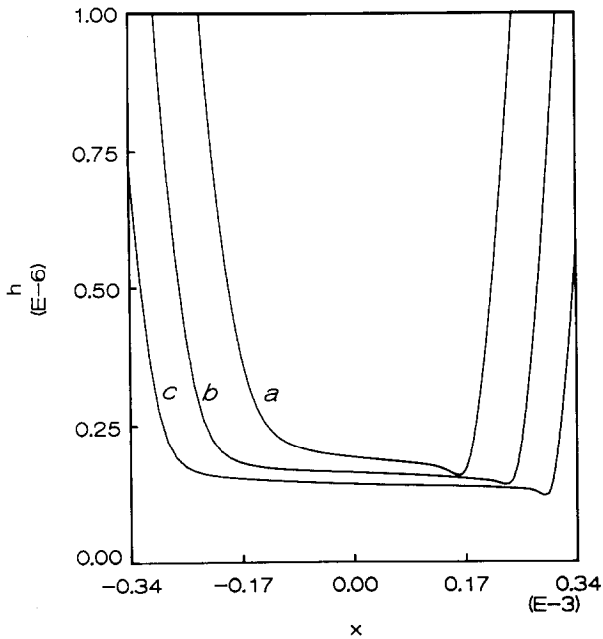

FIG. 11. The dependence of the film thickness on the loading. The film thickness belonging to the three pressure distribution shown in Fig. 10.
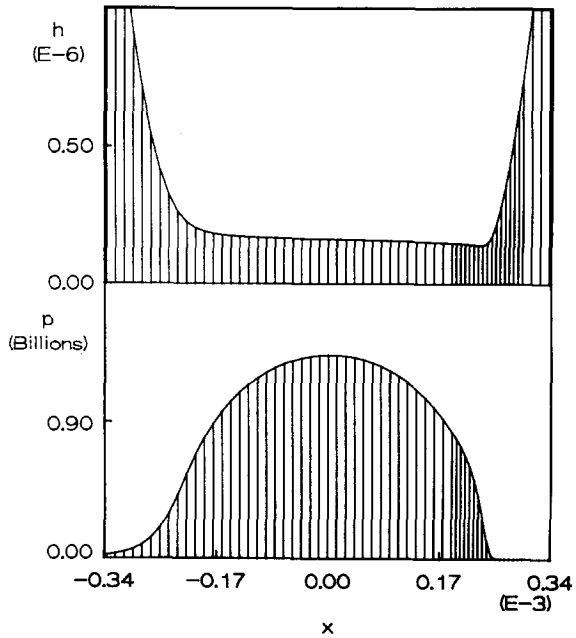
484

FIG. 12. The grid used for the calculation of the graphs 9B and 10B.
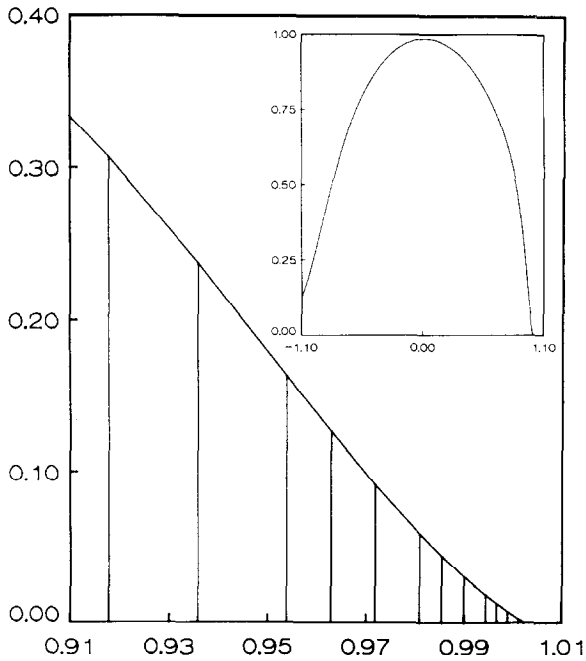

FIG. 13. The pressure p in the neighborhood of the cavitation boundary $x = b$. This computation is performed using a non-equidistant grid refinement. The x variable and p are scaled as in Fig. 9; $M \simeq 10$.

8. PRESSURE-DEPENDENT VISCOSITY

This section will deal with one extension of the previous analysis; the incorporation of a pressure-dependent viscosity like

$$\mu = \mu_0 \exp\left[\frac{\alpha p_0}{z}\left((1 + p/p_0)^z - 1\right)\right], \tag{38}$$

where (in SI units)

$$p_0 = 1.96 \times 10^8, \qquad \alpha p_0 = z(\log(\mu_0) + 9.67). \tag{39}$$

This relationship between μ and p was found empirically by Roelands [19] and is commonly referred to as Roelands' equation.

Concerning the variational structure of EHL, the pressure-dependence of μ has important consequences. Generally speaking, a set of differential equations that has a variational structure will lose this structure when constant parameters in the equations are changed into functions of quantities that are subject to variations.

Here, an ad hoc solution is be given: the viscosity μ in the time-discrete power (12) is evaluated at the previous time level $t = (i-1)\tau$,

$$\mu = \mu(p^{(i-1)}). \tag{40}$$

Then the Euler–Lagrange equations resulting from arbitrary variations at time $t = i\tau$ are not altered, since the relation between the viscosity and the pressure $p^{(i-1)}$ is not subject to variations. Moreover, the Euler–Lagrange equation (32) becomes linear in terms of the pressure $p^{(i)}$ and can be computed from the quadratic, convex minimization problem (28) as is described in Section 5.

Just as the approximation $h = h(p^{(i-1)})$ induces an error in the mass flux M_f, the effect of taking (40) instead of $\mu = \mu(p^{(i)})$ is similar. The additional error that is introduced in this way can be observed from the formulae,

$$M_f|_{\mu(p^{(i)})} = M_f|_{\mu(p^{(i-1)})} + \tau\, \partial_\mu M_f\, \partial_t \mu + \mathcal{O}(\tau^2)$$

$$= M_f|_{\mu(p^{(i-1)})} + \tau\, \frac{h^3\, \partial_x p}{12\mu}\, \alpha \left[1 + \frac{p}{p_0}\right]^{z-1} \partial_t p + \mathcal{O}(\tau^2).$$

This implies that $\mu(p^{(i)})$ in the integrated equation of continuity (19) can be replaced by $\mu(p^{(i-1)})$ if

$$\left| \tau\, \partial_x \frac{h^3\, \partial_x p}{12\mu}\, \alpha\, \partial_t p \left[1 + \frac{p}{p_0}\right]^{z-1} \right| \ll |\gamma\, \partial_t \mathcal{L}(p)|. \tag{41}$$

In terms of the characteristic dimensions introduced in Section 3 the flux M_f can be scaled by $\mathbf{v}\mathbf{h}$, and ∂_x by $\mathbf{1}^{-1}$. Furthermore,

$$|\mathcal{L}(p)| \geqslant \mathbf{1}\, |p|,$$

since $|\log|x-s|| > 1$. Inserting these scalings in (41) shows that Eq. (19) is (almost) not altered by adopting the approximation (40) if the time step τ is restricted to

$$\tau v \ll \frac{1}{\varepsilon\alpha}\frac{\gamma}{\varepsilon\alpha}\left[1 + \frac{p_{max}}{p_0}\right]^{1-z}, \tag{42}$$

where p_{max} is the maximum pressure occurring in the lubricant.

The above calculation resembles the approach described in Section 3. There, it was shown that the time step has to satisfy the condition (14), i.e., $\tau v \ll 1$, in order to justify the approximation $h = h(p^{(i-1)})$. Evaluating the viscosity at time $t = (i-1)\tau$ leads to (42). This requirement is satisfied if both (14) and

$$\frac{\gamma}{\varepsilon\alpha}\left[1 + \frac{p_{max}}{p_0}\right]^{1-z} = \mathcal{O}(1)$$

hold true. The latter requirement is fulfilled in cases like a steel–mineral oil contact. Indeed, such a lubricated contact can be characterized by the following values $\gamma \simeq 10^{-11}$, $\varepsilon \simeq 10^{-3}$. $\alpha \simeq 10^{-8}$, $z \simeq 0.7$, and the maximum pressure $p_{max} \simeq 10p_0$. This implies that, for such cases, (42) is always satisfied. Consequently, the linearization obtained by taking $\mu = \mu(p^{(i-1)})$ does not lead to an additional limitation of the time step τ. Figure 14 shows a numerical solution which is obtained in this way.
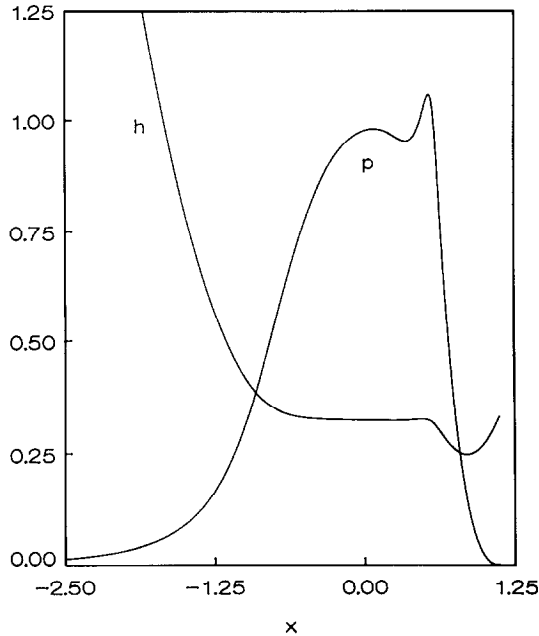

FIG. 14. The film thickness h of, and the pressure p in, a lubricant with a pressure-dependent viscosity. The x variable and the pressure are scaled as in Fig. 9; the film thickness is scaled with r/b_h^2. The dimensional numbers, as introduced in Ref. [18], are $M = 15$ and $L := \alpha[\mu_0\pi\gamma(\omega + v_0/r)]^{0.25}/(\pi\gamma) = 10$.

9. CONCLUSIONS

Calculations of the pressure in the lubricating film between a deformable cylinder and a rigid surface can be performed on a PC using only a few gridpoints and a small amount of run time. Here, the numerical algorithm for this elastohydrodynamic lubrication problem is based on the dynamic variation principle, so that mass flux defects cannot occur. The dynamic iteration can be speeded up by reducing the stiffness of the cylinder in several steps and by slowly increasing the loading on the cylinder. The number of calculations needed for one time-step is reduced by the introduction of a preconditioner.

ACKNOWLEDGMENTS

REFERENCES

1. D. DOWSON, *History of Tribology* (Longman, London, 1979), p. 30.
2. D. DOWSON AND G. R. HIGGINSON, *J. Mech. Eng. Sci.* **1**, 6 (1959).
3. K. P. OH, *Trans. J. Tribol.* **106** (1984).
4. B. J. HAMROCK AND B. O. JACOBSON, *Trans. ASME* **27**, 4 (1984).
5. A. A. LUBRECHT, W. E. TEN NAPEL, AND R. BOSMA, *J. Tribal.* **108**, 551 (1986).
6. H. SCHLICHTING, *Boundary Layer Theory* (6th ed., McGraw–Hill, New York, 1968).
7. R. VERSTAPPEN AND E. VAN GROESEN, *J. Tribal.* **111**, 108 (1989).
8. E. VAN GROESEN AND R. VERSTAPPEN, *Int. J. Eng. Sci.* **28**, 99 (1990).
9. J. E. MARSDEN AND T. J. R. HUGHES, *Mathematical Foundations of Elasticity* (Prentice–Hall, Englewood Cliffs, NJ, 1983).
10. A. Z. SZERI, *Tribology: Friction, Lubrication and Wear* (Hemisphere, Washington, DC, 1980).
11. A. E. H. LOVE, *A Treatise on the Mathematical Theory of Elasticity* (4th ed., Cambridge Univ. Press, Cambridge, UK, 1952).
12. R. VERSTAPPEN, Ph.D. thesis, University of Twente, Enschede, The Netherlands, 1989 (unpublished).
13. P. R. GOGLIA, Ph.D. thesis, University of Illinois, Urbana-Champaign, 1982 (unpublished).
14. R. LEE AND B. J. HAMROCK, *J. Tribal.* **111**, 1 (1989).
15. C. E. FRÖBERG, *Introduction to Numerical Analysis* (Addison–Wesley, Reading, MA, 1965), p. 97.
16. L. CHANG, T. F. CONRY, AND C. CUSANO, *J. Tribol.* **111**, 193 (1989).
17. P. CASTLE AND D. DOWSON, *Proc. Inst. Mech. Eng.* **185**, 131 (1972).
18. H. MOES, *Proc. Inst. Mech. Eng.* **180**, 244 (1965).
19. C. J. R. ROELANDS, Ph.D. thesis, Technical University of Delft, Delft, The Netherlands, 1966 (unpublished).